

Published in final edited form as:

*Biochim Biophys Acta*. 2012 April ; 1817(4): 666–671. doi:10.1016/j.bbabi.2011.11.010.

## The Rate-Limiting Step in O<sub>2</sub> Reduction by Cytochrome *ba*<sub>3</sub> from *Thermus thermophilus*

Tsuyoshi Egawa<sup>§</sup>, Ying Chen<sup>||</sup>, James A. Fee<sup>||</sup>, Syun-Ru Yeh<sup>§</sup>, and Denis L. Rousseau<sup>§,\*</sup>

<sup>§</sup>Department of Physiology and Biophysics, Albert Einstein College of Medicine, Bronx, NY

<sup>||</sup>Department of Molecular Biology, The Scripps Research Institute, La Jolla, 92037 CA

### Abstract

Cytochrome *ba*<sub>3</sub> (*ba*<sub>3</sub>) of *Thermus thermophilus* (*T. thermophilus*) is a member of the heme-copper oxidase family, which has a binuclear catalytic center comprised of a heme (heme *a*<sub>3</sub>) and a copper (Cu<sub>B</sub>). The heme-copper oxidases generally catalyze the four electron reduction of molecular oxygen in a sequence involving several intermediates. We have investigated the reaction of the fully reduced *ba*<sub>3</sub> with O<sub>2</sub> using stopped-flow techniques. Transient visible absorption spectra indicated that a fraction of the enzyme decayed to the oxidized state within the dead time (~1 ms) of the stopped-flow instrument, while the remaining amount was in a reduced state that decayed slowly ( $k = 400 \text{ s}^{-1}$ ) to the oxidized state without accumulation of detectable intermediates. Furthermore, no accumulation of intermediate species at 1 ms was detected in time resolved resonance Raman measurements of the reaction. These findings suggest that O<sub>2</sub> binds rapidly to heme *a*<sub>3</sub> in one fraction of the enzyme and progresses to the oxidized state. In the other fraction of the enzyme, O<sub>2</sub> binds transiently to a trap, likely Cu<sub>B</sub>, prior to its migration to heme *a*<sub>3</sub> for the oxidative reaction, highlighting the critical role of Cu<sub>B</sub> in regulating the oxygen reaction kinetics in the oxidase superfamily.

### Keywords

Cytochrome oxidase; bioenergetics; Raman scattering; stopped flow

## 1. Introduction

The heme-copper oxidase family of enzymes catalyzes the four electron reduction of molecular oxygen to water, concomitantly producing a proton gradient across the associated membranes. The chemical intermediates formed during the catalytic turnover have been clarified by studies of a variety of mammalian and bacterial *aa*<sub>3</sub> enzymes, which show a progressive **R**→**A**→**P**→**F**→**O** transition (where **R**, **A**, **P/F** and **O** are the fully-reduced, O<sub>2</sub>-bound, ferryl and oxidized states of the enzymes, respectively) (Fig. S1 in Supplementary Data). The cytochrome *ba* from *Thermus thermophilus* shares the architecture of the catalytic sites with *aa*<sub>3</sub> type of enzymes [1], although in this oxidase Cu<sub>B</sub> is known to have

© 2011 Elsevier B.V. All rights reserved.

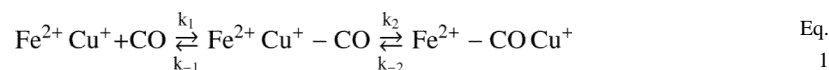
\*To whom correspondence should be addressed. Tel. 718 430-4264, Fax. 718 430-8808, denis.rousseau@einstein.yu.edu.

Supplementary data

Supplementary data associated with this article can be found in the online version.

**Publisher's Disclaimer:** This is a PDF file of an unedited manuscript that has been accepted for publication. As a service to our customers we are providing this early version of the manuscript. The manuscript will undergo copyediting, typesetting, and review of the resulting proof before it is published in its final citable form. Please note that during the production process errors may be discovered which could affect the content, and all legal disclaimers that apply to the journal pertain.

an unusually high affinity towards carbon monoxide (CO), with a  $K_a$  of  $10^4 \text{ M}^{-1}$  with respect to  $87 \text{ M}^{-1}$  of the bovine  $aa_3$  enzyme [2, 3]. Thus, whereas the reaction of the enzyme with CO follows the same pathway as other oxidases as illustrated in Eq. 1,  $k_{-2}$  is about 30-fold larger than that in bovine cytochrome c oxidase (CcO) [2] and consequently the CO-bound Cu species is readily detected under equilibrium conditions [1, 4].



However, although the CO-binding has been heavily investigated in  $ba_3$ , it has not been determined if the  $\text{Cu}_B$  affinity for  $\text{O}_2$  is also unusual, resulting in  $\text{O}_2$  reduction kinetics that are distinct from that in other heme-copper oxidases.

Despite several studies, the reaction kinetics of the  $ba_3$  enzyme with  $\text{O}_2$  is controversial [2, 3, 5]. With stopped-flow optical absorption, Giuffr  *et al.* observed a single exponential kinetic phase at  $20 \text{ }^\circ\text{C}$ , with a rate constant of  $200 \text{ s}^{-1}$ , which is significantly slower than that of the  $aa_3$  enzymes ( $700\text{--}1000 \text{ s}^{-1}$ ) [2]. They assigned the phase to the **F**  $\rightarrow$  **O** transition, which is usually the rate-limiting in the single turnover reaction of other heme-copper oxidases. In contrast, using the CO photolysis method, Smirnova *et al.* reported that the reaction rate of the **F**  $\rightarrow$  **O** step ( $1100 \text{ s}^{-1}$  at  $22 \text{ }^\circ\text{C}$ ) was comparable to that in the  $aa_3$  oxidases, and only a minor component (10–13 %) showed a slower reaction rate ( $\sim 200 \text{ s}^{-1}$ ) [5]. Similarly, using CO photolysis combined with electrometric measurements at  $23 \text{ }^\circ\text{C}$ , Siletsky *et al.* showed that the major kinetic phase of the reaction associated with the **F**  $\rightarrow$  **O** transition displayed a rate constant of  $1300 \text{ s}^{-1}$ , while the minor ( $\sim 3\%$ ) slower component showed a rate constant of  $400 \text{ s}^{-1}$  [3].

In this study, we sought to clarify the origin of the aforementioned differences, to gain a better understanding of the kinetics of the  $ba_3$  reaction, and to examine whether the  $\text{Cu}_B$  affinity for  $\text{O}_2$  plays a key role in the catalytic turn-over of  $ba_3$ . To this end, we re-examined the absorption changes upon stopped-flow mixing of  $\text{O}_2$  with the reduced enzyme, and studied the reaction with time resolved resonance Raman spectroscopy.

## 2. Material and Methods

### 2.1 Materials

Cytochrome  $ba_3$  was prepared as described previously [6]. The protein was concentrated to  $\sim 100 \text{ } \mu\text{M}$  in  $10 \text{ mM}$  potassium phosphate buffer,  $\text{pH } 7.5$ , with  $1 \text{ mM}$  dodecylmaltoide. The samples were stored at  $4 \text{ }^\circ\text{C}$ . Bovine CcO was isolated and purified as described [7] and stored at  $77 \text{ K}$ . The mixed valence F (mvF) preparation was made by mixing the bovine CcO with  $\text{H}_2\text{O}_2$  [8] and the mixed valence P (mvP) sample was prepared by exposing the enzyme to a 1:1 mixture of CO and  $\text{O}_2$  [9] at the room temperature.

### 2.2 Spectroscopic measurements

Time-resolved UV-visible absorption spectra were measured at  $8 \text{ }^\circ\text{C}$  on an Applied Photophysics PiStar system equipped with a stopped flow apparatus, a photodiode array detection system, an anaerobic accessory and a temperature control unit. The time zero ( $t = 0$ ) point and its uncertainty of the stopped flow system were determined employing a test reaction comprised of 2,6-dichlorophenol-indophenol and ascorbic acid [10]; the uncertainty was determined to be at the limit of the minimum sampling time ( $1.4 \text{ ms}$ ) of the system. Thus we are unable to determine precisely the relative amplitude of the missing early phase. The  $ba_3$  sample was fully reduced by a slightly excess amount of sodium dithionite, and mixed with an  $\text{O}_2$  saturated buffer in the stopped flow apparatus at a 1:1 ratio. Alternatively,

the enzyme (40  $\mu\text{M}$ ) was reduced with ascorbate (2 mM) and N-methyl phenazinium methyl sulfate (PMS) (5  $\mu\text{M}$ ). Similar results were obtained with both reductants. The concentrations of  $ba_3$  and  $\text{O}_2$  after the mixing were 20 and  $\sim 600$   $\mu\text{M}$ , respectively.

Time-resolved resonance Raman spectra were measured using a home-made continuous flow apparatus [11]. Raman scattering was excited by the 413.1 nm line of a  $\text{Kr}^+$  laser (Spectraphysics, BeamLock 2080), and collected into a Spex 1.25 m polychromator equipped with a charge-coupled device detector (Princeton Instruments, Model 1100PB). The spectra were calibrated with the Raman bands of metMb, for which the accurate band positions were determined by independent experiments using a spinning cell system and indene as the Raman frequency standard.

### 3. Results

#### 3.1 Stopped Flow Optical Absorption Measurements

As shown in Fig. 1A and C, the fully reduced  $ba_3$  enzyme (**R**) has a Soret band at 426 nm with a shoulder at  $\sim 440$  nm (from the low spin heme  $b$  and the high spin heme  $a_3$ , respectively) and a visible band at 558 nm (from reduced heme  $b$ ) [3, 5]. The weak shoulder at  $\sim 590$  nm, attributed to a low spin heme  $a_3$  species, suggest a micro heterogeneity in the enzyme sample [12], perhaps due to the partial absence of  $\text{Cu}_B$  resulting in formation of bis-His heme  $a_3$  [6]. Immediately following the mixing of the fully reduced enzyme (**R**) with  $\text{O}_2$ -saturated buffer, the Soret band shifted to  $\sim 422$  nm, and decreased in intensity, along with a decrease in intensity of the visible band at 558 nm. As the reaction progressed, the 422 nm band shifted to 417 nm, accompanied by further reduction of the intensity of the visible band, cumulating in a spectrum similar to that of the fully oxidized enzyme [13], **O**, at 280 ms. The small residual intensity at 558 nm indicates that the reaction has not yet reached completion. The difference spectrum obtained by subtracting the **O** spectrum from the 1.4 ms spectrum has a peak and trough at 426 and 408 nm, respectively, which was assigned by Giuffrè *et al.*, as the **F minus O** difference spectrum[2].

The kinetic traces at 426 nm ( $\lambda_{\text{max}}$  of the **R** state) and 558 nm ( $\lambda_{\text{max}}$  of the reduced heme  $b$ ) shown in Fig. 1B and D are best-fitted with a single exponential function with a rate constant of  $400 \text{ s}^{-1}$ . In both cases, the absorbance at  $t=0$  (the upright triangle) obtained by extrapolating the kinetic trace to time zero is lower than that of the **R** state (the inverted triangle), indicating the existence of an additional kinetic phase unresolved with our instrument. However, the amplitude of the missing phase cannot be precisely determined with our current instrumentation. These optical changes, occurring after 1.4 ms, may be compared to those reported by Sundi *et al.* between  $10^{-6}$  and  $10^{-2}$  s [14].

#### 3.2 Resonance Raman Measurements

To further explore the identity of the 1.4 ms intermediate, we measured the RR spectrum (Fig. 2) of the sample at 1.0 ms following the initiation of the oxygen reaction in a home-made continuous-flow mixer [11]. The RR bands of  $ba_3$  have been previously assigned [15, 16]. Among them, a porphyrin core vibration mode in the  $1350\text{--}1400 \text{ cm}^{-1}$  region,  $\nu_4$ , is especially useful for the determination of the oxidation states of the two heme centers. The  $\nu_4$  mode, which is sensitive to the electron density of the heme irons, exhibits systematic frequency shifts in the following order: ferrous < ferric < ferryl ( $a_3^{4+}=\text{O}^{2-}$ ) [17–19]. As a reference, we measured the  $\nu_4$  bands of the ferryl derivative of the bovine  $aa_3$  oxidase, with 413.1 nm excitation, the same as that used to obtain the spectrum of the  $ba_3$  intermediate. The data show that the frequency of the  $\nu_4$  band of the ferryl species derived from either mixed valence **F** or mixed valence **P** intermediate (each of which is comprised of a ferryl

heme  $a_3$  ( $a^{3+}a_3^{4+=O^{2-}}$ ) [20, 21] and a ferric heme  $a$ ) was higher than that of the oxidized enzyme (Fig. S2 in Supplementary Data).

The RR spectrum of the intermediate at 1.0 ms exhibits  $\nu_4$  modes at  $\sim 1358$  and  $\sim 1372$   $\text{cm}^{-1}$  (Fig. 3A), which are assigned to the **R** and **O** states of the enzyme, respectively. The  $\nu_4$  mode assigned to the **O** state is identical to that of the oxidized enzyme shown in Fig. 3A, and is similar to that of the published data [16]. To confirm the assignment of the  $1372$   $\text{cm}^{-1}$  mode to the **O** state, we calculated a series of difference spectra by subtracting the **O** spectrum from the 1 ms spectrum with various ratios (Fig. 3B). None of these difference spectra showed derivative-like shapes as that observed in the **O** minus **F** spectrum of the bovine  $aa_3$  enzyme (Fig. S2 in Supplementary Data), indicating that the intermediate is not **F** or any other ferryl species. Consistent with the absence of evidence for a ferryl species, no oxygen sensitive lines could be detected in the low frequency RR spectrum of the intermediate based on  $^{16}\text{O}_2$ - $^{18}\text{O}_2$  isotopic substitution experiments (Fig. S3 in Supplementary Data).

In contrast to the behavior of the oxidized component, if the **R** spectrum is subtracted from the 1 ms spectrum with various ratios (Fig. 3C), derivative-like shapes (with peak and trough at  $1360$  and  $1353$   $\text{cm}^{-1}$ , respectively) emerge. The fact that a clean cancellation of the  $\nu_4$  band at  $1358$   $\text{cm}^{-1}$  could not be achieved via the subtraction procedure reveals the presence of a new species, which exhibits its  $\nu_4$  band at a slightly higher frequency than the  $\nu_4$  of the **R** state at  $1358$   $\text{cm}^{-1}$ . It should be noted that the derivative shape indicates a small band shift of  $\nu_4$  to higher frequency but the positions of the peak and trough in the spectrum do not indicate a  $7$   $\text{cm}^{-1}$  shift but rather they depend on the center frequencies, bandwidths and intensities of the original bands [22]. Nonetheless, it is certain that the  $\nu_4$  frequency of the intermediate is close to that of the equilibrium **R** state, indicating that the hemes remain reduced but, importantly, their structures are perturbed.

Additional information on the properties of the mixture of the **O** state and the perturbed **R** state present at  $\sim 1$  ms is provided by the other lines in the resonance Raman spectrum (Fig. 2). The spectrum may be simulated by a mixture of the equilibrium **R** and **O** states with one interesting difference. The high spin marker line  $\nu_3$  from reduced heme  $a_3$  at  $1470$   $\text{cm}^{-1}$  is absent in the intermediate spectrum indicating that the structure of the **R** state in the intermediate has low spin character.

## 4.0 Discussion

### 4.1 Assignment of the intermediate structure

Taken together the data reported here suggest that the 1 ms intermediate is a mixture of the fully reduced enzyme with a perturbed **R** structure (named **R'** hereafter) and the fully oxidized enzyme (**O**), without any evidence for the formation of ferryl species. The data shown in Fig. 1A support this conclusion as it indicates that heme  $b$  in the intermediate is partially oxidized, while the **F** species of the  $ba_3$  enzyme has been shown to have a reduced rather than an oxidized heme  $b$  [3, 5]. Moreover, the 610 nm band was not observable in the 1.4 ms minus **O** spectrum shown in Fig. 1C, despite the fact that in the **F** minus **O** spectrum obtained from CO photolysis measurements [3, 5] the intensity of the 610 nm band is about 70% of the 558 nm band originating from heme  $b^{2+}$  [3]. It is noted that although the 1.4 ms spectrum has a weak shoulder at  $\sim 610$  nm, it is assigned to the 612 nm band of the residual **R** state.

As an additional test, we simulated the visible spectrum of the intermediate by a linear combination of the **R** and **O** spectra. The best fitted spectrum, accurately reproduced the intermediate spectrum, with negligible residuals (Fig. 1C). Thus, the difference between this

linear combination and the 1.4 ms spectrum (thick dotted trace in Fig. 1C) is essentially featureless, confirming that the 1.4 ms minus O state spectrum (Fig. 1A) can be fully accounted for by an **R'** minus **O** difference spectrum, if the visible spectrum of **R'** is approximately the same as that of **R**. In summary, our experimental findings show that the **R** state  $ba_3$  decayed to the **O** state upon reacting with  $O_2$  without detectable build up of discrete intermediates in the stopped-flow time range. Although there were minor differences, the spectroscopic characteristics of the reduced state (**R'**) present at ~1 ms were very close to those of the initial **R** state.

The observation of two components in the oxygen reaction at 1 ms, one of which is a perturbed reduced state indicates that the  $O_2$  has interacted with the enzyme in **R'** and is likely trapped in a docking site along its pathway to the heme  $a_3$  iron atom. In addition to the obvious possibility of  $Cu_B$ , other potential ligand docking sites have been identified in the past by crystallographic studies of Xe and Kr binding and by CO photolysis studies. In the latter experiments, reported by Varotsis and coworkers,  $B_0$  and  $B_1$  CO docking sites were detected, analogous to such sites reported in myoglobin [23]. Interestingly, the penultimate  $O_2$  binding site (Xe1) determined from the crystallographic studies [24] lies close (~5 Å) from one of the heme propionates and accordingly could be the same site as that determined in the CO photolysis measurements[1].

To assess each of the potential binding sites we consider the properties of the putative  $O_2$  channel and the potential docking sites that lie in the channel. Crystallographic studies determined that  $O_2$  could enter through a large unrestricted hydrophobic tunnel that extended all the way into the space between the heme  $a_3$  iron and  $Cu_B$  [24, 25]. Therefore the  $O_2$  would have no obstruction for gaining access to the binuclear center [25]. As the non- $Cu_B$  putative docking sites are located along this pathway, their kinetics properties must be considered. The CO off-rate kinetics of the  $B_1$  and  $B_0$  sites were determined by Varotsis and coworkers to be 85 and 110  $\mu s$ , respectively [23]. Therefore, the CO off-rates of the docking sites (~100  $\mu s$ ) are much faster than the decay of **R'** (~2.5 ms). On the other hand it is well documented that CO binds to  $Cu_B$  and forms a metastable adduct in  $ba_3$  in which the transfer rate of CO from  $Cu_B$  to the heme iron is quite slow (35 ms,  $k_2=28.6 s^{-1}$ ) [1]. This is slower than the observed rate of  $400 s^{-1}$  (2.5 ms) in our data. Therefore our observed rate is too slow as compared to the non- $Cu_B$  sites and too fast as compared to the  $Cu_B$  site. However, in bovine CcO the transfer rate for CO from  $Cu_B$  to heme  $a_3$  ( $k_2$ ) is  $\sim 10^3 s^{-1}$  [26] but it is much faster for  $O_2$  ( $\sim 10^5 s^{-1}$ ) [27, 28]. By comparison, we would expect that the  $O_2$  transfer rate in  $ba_3$  would also be significantly faster than the CO transfer rate, making  $Cu_B$  the most likely docking site for the  $O_2$ .

## 4.2 Reaction Scheme

Based on the above considerations we postulate that  $Cu_B$  is the metastable binding site for  $O_2$  and the oxygen reaction follows the bifurcated reaction mechanism illustrated in Figure 4. Following the initiation of the reaction, in one fraction of the  $ba_3$  enzyme,  $O_2$  binds rapidly to heme  $a_3$  (with a rate constant of  $k_3$ ), leading to an  $O_2$ -complex (the **A** state), which rapidly decays to the oxidized **O** state (with a rate constant  $>1,000 s^{-1}$ ), accounting for the missing phase in the stopped-flow data shown in Fig. 1. In the other fraction of the enzyme,  $O_2$  binds to  $Cu_B$ , with a rate constant of  $k_1$ , which leads to a metastable intermediate, **R'**, with spectroscopic properties slightly perturbed from those of the equilibrium **R** state. The **R'** state subsequently converts to the **A** state via an intramolecular ligand transfer from  $Cu_B$  to heme  $a_3$ , with a rate constant of  $400 s^{-1}$ ; the **A** state ultimately decays to the **O** state without populating any detectable intermediates. On the basis of this mechanism, the rate-limiting step of the reaction is the intramolecular ligand transfer from  $Cu_B$  to heme  $a_3$ , manifesting the important role of  $Cu_B$  in regulating the oxygen reaction kinetics of the  $ba_3$  enzyme. It is noteworthy that although  $O_2$  also binds to  $Cu_B$  in  $aa_3$

enzymes [29], due to its short lifetime, its influence on the oxygen reaction kinetics is not as prominent as in *ba*<sub>3</sub>.

The structural basis for the two distinct phases of the oxygen reaction of the *ba*<sub>3</sub> enzyme remains to be further investigated. Native gel electrophoresis on *ba*<sub>3</sub> showed only a single band. However, this does not mean that there is no conformational heterogeneity in the *ba*<sub>3</sub> protein, as conformational differences in the region of the active site would not be expected to be separated on a native gel. Indeed, FT-IR studies of the CO-bound *ba*<sub>3</sub> indicate that the heme-CO moiety resides in three distinct conformations [1, 4]. Our preliminary resonance Raman experiments also demonstrate the presence of at least two active site conformers of the CO-bound *ba*<sub>3</sub> (T. Egawa et al., unpublished results). Analogous heme-CO conformers have also been seen in other terminal oxidases, and they are classified into either  $\alpha$  or  $\beta$  forms, depending on the frequencies of the iron-CO and C-O stretching modes [30–32]. The relative populations of such two conformers have been correlated with the catalytic activity of the enzyme [32]. Interestingly, in *ba*<sub>3</sub>, the multiple structures appear to fall in the range of only the  $\alpha$  conformation in the other proteins (T. Egawa et al., unpublished data). MCD studies have also revealed the heterogeneity in the CO-adduct of the *ba*<sub>3</sub> enzyme [12]. Thus the presence of multiple conformations in terminal oxidases is well established and the results reported here demonstrate the functional consequences of the heterogeneity.

## 5. Conclusion

The data reported here indicate that the high affinity of Cu<sub>B</sub> toward O<sub>2</sub> plays a pivotal role in regulating the oxygen reaction kinetics of the *ba*<sub>3</sub> enzyme. They also account for the discrepancy in the oxygen reaction kinetic data resulting from stopped-flow mixing and CO-photolysis studies. It is conceivable that, in the photolysis experiments, the photolyzed CO transiently occupies the Cu<sub>B</sub> site [3, 5], and prevents the reaction from being kinetically trapped in the **R'** state, thereby accounting for the major phase with a rate of  $>1,000\text{ s}^{-1}$ . From a physiological point of view, the high affinity of Cu<sub>B</sub> toward O<sub>2</sub> in the *ba*<sub>3</sub> enzyme is plausibly beneficial for the survival of the *T. thermophilus* bacterium under conditions of reduced oxygen tension as it increases the efficiency of the enzyme to utilize O<sub>2</sub> for energy production.

## Supplementary Material

Refer to Web version on PubMed Central for supplementary material.

## Acknowledgments

Funding for this work was provided by the National Institutes of Health Grants GM074982 and GM098799 to D.L.R. and GM035342 to J.A.F. and the National Science Foundation Grant NSF0956358 to S.-R.Y.

## ABBREVIATIONS

<i>ba</i> <sub>3</sub>	Cytochrome <i>ba</i> <sub>3</sub> from <i>Thermusthermophilus</i>
RR	Resonance Raman

## References

1. Koutsoupakis K, Stavarakis S, Pinakoulaki E, Soulimane T, Varotsis C. Observation of the equilibrium Cu<sub>B</sub>-CO complex and functional implications of the transient heme a<sub>3</sub> propionates in cytochrome *ba*<sub>3</sub>-CO from *Thermus thermophilus*. Fourier transform infrared (FTIR) and time-resolved step-scan FTIR studies. *J Biol Chem.* 2002; 277:32860–32866. [PubMed: 12097331]



2. Giuffre A, Forte E, Antonini G, D'Itri E, Brunori M, Soulimane T, Buse G. Kinetic properties of ba<sub>3</sub> oxidase from *Thermus thermophilus*: effect of temperature. *Biochemistry*. 1999; 38:1057–1065. [PubMed: 9894002]
3. Siletsky SA, Belevich I, Jasaitis A, Konstantinov AA, Wikstrom M, Soulimane T, Verkhovsky MI. Time-resolved single-turnover of ba<sub>3</sub> oxidase from *Thermus thermophilus*. *Biochim Biophys Acta*. 2007; 1767:1383–1392. [PubMed: 17964277]
4. Pinakoulaki E, Ohta T, Soulimane T, Kitagawa T, Varotsis C. Simultaneous resonance Raman detection of the heme a<sub>3</sub>-Fe-CO and CuB-CO species in CO-bound ba<sub>3</sub>-cytochrome c oxidase from *Thermus thermophilus*. Evidence for a charge transfer CuB-CO transition. *J Biol Chem*. 2004; 279:22791–22794. [PubMed: 15066990]
5. Smirnova IA, Zaslavsky D, Fee JA, Gennis RB, Brzezinski P. Electron and proton transfer in the ba(3) oxidase from *Thermus thermophilus*. *J Bioenerg Biomembr*. 2008; 40:281–287. [PubMed: 18752061]
6. Chen Y, Hunsicker-Wang L, Pacoma RL, Luna E, Fee JA. A homologous expression system for obtaining engineered cytochrome ba<sub>3</sub> from *Thermus thermophilus* HB8. *Protein Expr Purif*. 2005; 40:299–318. [PubMed: 15766872]
7. Yoshikawa S, Choc MG, O'Toole MC, Caughey WS. An infrared study of CO binding to heart cytochrome c oxidase and hemoglobin A. Implications re O<sub>2</sub> reactions. *J Biol Chem*. 1977; 252:5498–5508. [PubMed: 195952]
8. Bickar D, Bonaventura J, Bonaventura C. Cytochrome c oxidase binding of hydrogen peroxide. *Biochemistry*. 1982; 21:2661–2666. [PubMed: 6284205]
9. Ji H, Yeh SR, Rousseau DL. Structural characterization of the [Pco/o(2)] compound of cytochrome c oxidase. *FEBS Lett*. 2005; 579:6361–6364. [PubMed: 16263119]
10. Tonomura B, Nakatani H, Ohnishi M, Yamaguchi-Ito J, Hiromi K. Test reactions for a stopped-flow apparatus. Reduction of 2,6-dichlorophenolindophenol and potassium ferricyanide by L-ascorbic acid. *Anal Biochem*. 1978; 84:370–383. [PubMed: 626384]
11. Takahashi S, Yeh SR, Das TK, Chan CK, Gottfried DS, Rousseau DL. Folding of cytochrome c initiated by submillisecond mixing. *Nat Struct Biol*. 1997; 4:44–50. [PubMed: 8989323]
12. Goldbeck RA, Einarsdottir O, Dawes TD, O'Connor DB, Surerus KK, Fee JA, Kliger DS. Magnetic circular dichroism study of cytochrome ba<sub>3</sub> from *Thermus thermophilus*: spectral contributions from cytochromes b and a<sub>3</sub> and nanosecond spectroscopy of CO photodissociation intermediates. *Biochemistry*. 1992; 31:9376–9387. [PubMed: 1327113]
13. Farver O, Chen Y, Fee JA, Pecht I. Electron transfer among the CuA-, heme b- and a<sub>3</sub>-centers of *Thermus thermophilus* cytochrome ba<sub>3</sub>. *FEBS Lett*. 2006; 580:3417–3421. [PubMed: 16712843]
14. Szundi I, Funatogawa C, Fee JA, Soulimane T, Einarsdottir O. CO impedes superfast O<sub>2</sub> binding in ba<sub>3</sub> cytochrome oxidase from *Thermus thermophilus*. *Proc Natl Acad Sci U S A*. 107:21010–21015. [PubMed: 21097703]
15. Gerscher S, Hildebrandt P, Buse G, Soulimane T. The active site structure of ba<sub>3</sub> oxidase from *Thermus thermophilus* studied by resonance raman spectroscopy. *Biospectroscopy*. 1999; 5:S53–63. [PubMed: 10512538]
16. Oertling WA, Surerus KK, Einarsdottir O, Fee JA, Dyer RB, Woodruff WH. Spectroscopic characterization of cytochrome ba<sub>3</sub>, a terminal oxidase from *Thermus thermophilus*: comparison of the a<sub>3</sub>/CuB site to that of bovine cytochrome aa<sub>3</sub>. *Biochemistry*. 1994; 33:3128–3141. [PubMed: 8130228]
17. Chuang WJ, Heldt J, Van Wart HE. Resonance Raman spectra of bovine liver catalase compound II. Similarity of the heme environment to horseradish peroxidase compound II. *J Biol Chem*. 1989; 264:14209–14215. [PubMed: 2547789]
18. Kitagawa T, Ozaki Y. Infrared and Raman spectra of metalloporphyrins. *Struct Bonding*. 1987; 64:71–114.
19. Spiro TG. Resonance Raman spectroscopy as a probe of heme protein structure and dynamics. *Adv Protein Chem*. 1985; 37:111–159. [PubMed: 2998161]
20. Branden G, Gennis RB, Brzezinski P. Transmembrane proton translocation by cytochrome c oxidase. *Biochim Biophys Acta*. 2006; 1757:1052–1063. [PubMed: 16824482]

21. Kitagawa T, Ogura T. Time-resolved resonance Raman study of dioxygen reduction by cytochrome c oxidase. *Pure & Appl Chem.* 1998; 70:881–888.
22. Rousseau DL. Raman difference spectroscopy as a probe of biological molecules. *J Raman Spectrosc.* 1981; 10:94–99.
23. Koutsoupakis C, Soulimane T, Varotsis C. Docking site dynamics of ba3-cytochrome c oxidase from *Thermus thermophilus*. *J Biol Chem.* 2003; 278:36806–36809. [PubMed: 12851397]
24. Luna VM, Chen Y, Fee JA, Stout CD. Crystallographic studies of Xe and Kr binding within the large internal cavity of cytochrome ba3 from *Thermus thermophilus*: structural analysis and role of oxygen transport channels in the heme-Cu oxidases. *Biochemistry.* 2008; 47:4657–4665. [PubMed: 18376849]
25. Liu B, Chen Y, Doukov T, Soltis SM, Stout CD, Fee JA. Combined microspectrophotometric and crystallographic examination of chemically reduced and X-ray radiation-reduced forms of cytochrome ba3 oxidase from *Thermus thermophilus*: structure of the reduced form of the enzyme. *Biochemistry.* 2009; 48:820–826. [PubMed: 19140675]
26. Woodruff WH. Coordination dynamics of heme-copper oxidases. The ligand shuttle and the control and coupling of electron transfer and proton translocation. *J Bioenerg Biomembr.* 1993; 25:177–188. [PubMed: 8389750]
27. Oliveberg M, Malmstrom BG. Reaction of dioxygen with cytochrome c oxidase reduced to different degrees: indications of a transient dioxygen complex with copper-B. *Biochemistry.* 1992; 31:3560–3563. [PubMed: 1314642]
28. Verkhovskiy MI, Morgan JE, Wikstrom M. Oxygen binding and activation: early steps in the reaction of oxygen with cytochrome c oxidase. *Biochemistry.* 1994; 33:3079–3086. [PubMed: 8130222]
29. Blackmore RS, Greenwood C, Gibson QH. Studies of the primary oxygen intermediate in the reaction of fully reduced cytochrome oxidase. *J Biol Chem.* 1991; 266:19245–19249. [PubMed: 1655779]
30. Das TK, Tomson FL, Gennis RB, Gordon M, Rousseau DL. pH-dependent structural changes at the Heme-Copper binuclear center of cytochrome c oxidase. *Biophys J.* 2001; 80:2039–2045. [PubMed: 11325707]
31. Egawa T, Lin MT, Hosler JP, Gennis RB, Yeh SR, Rousseau DL. Communication between R481 and Cu(B) in cytochrome bo(3) ubiquinol oxidase from *Escherichia coli*. *Biochemistry.* 2009; 48:12113–12124. [PubMed: 19928831]
32. Ji H, Das TK, Puustinen A, Wikstrom M, Yeh SR, Rousseau DL. Modulation of the active site conformation by site-directed mutagenesis in cytochrome c oxidase from *Paracoccus denitrificans*. *J Inorg Biochem.* 2010; 104:318–323. [PubMed: 20056281]



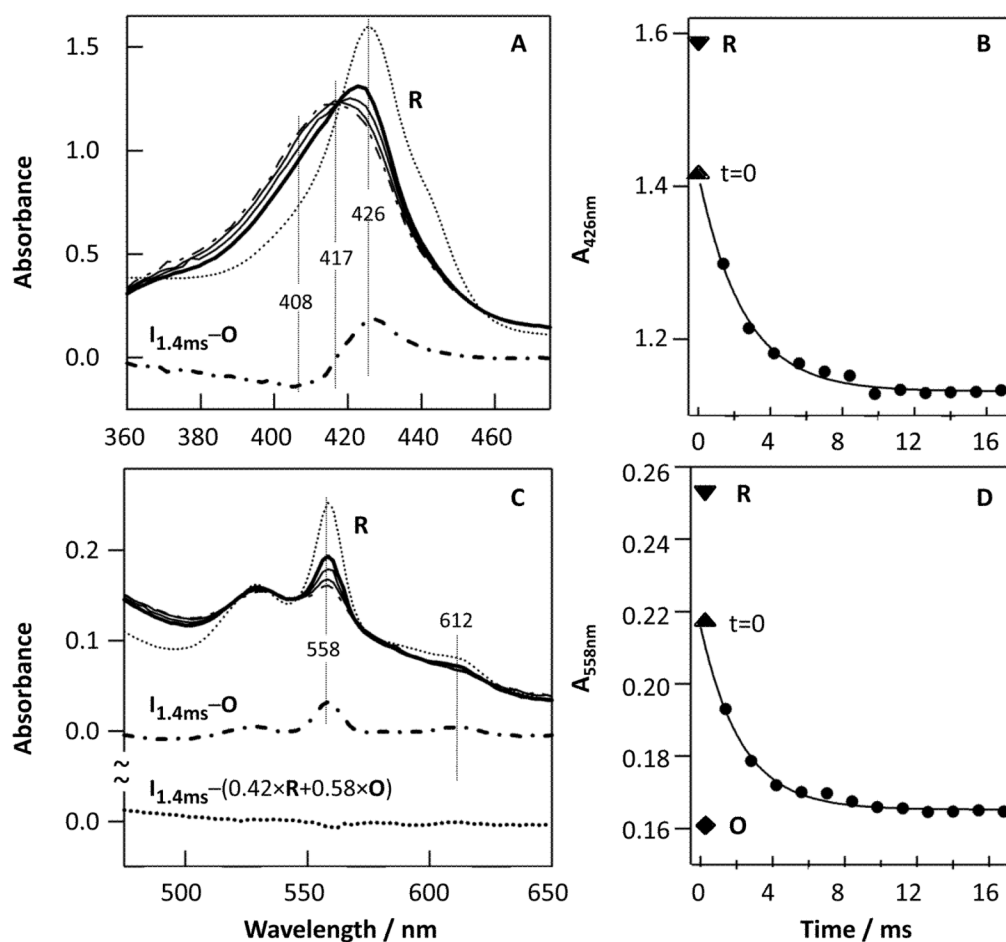


**Figure 1.**

Optical absorption spectra obtained following 1:1 mixing of the fully reduced  $ba_3$  (**R**) with  $O_2$ -saturated buffer in a stopped-flow instrument (A, C) and the associated kinetic traces at 426 nm (B) and 558 nm (D). The spectra in (A) and (C) were obtained at 1.4 ms (thick solid line), 2.8 and 7.0 ms (thin solid lines) and 280 ms (dot-dashed line); the thick dot-dashed lines were calculated from  $I_{1.4\text{ms}} - O$ , where  $I_{1.4\text{ms}}$  and  $O$  are the intermediate and oxidized spectra obtained at 1.4 and 280 ms, respectively. The thin dotted lines in (A) and (C) are the **R** state spectrum. The thick dotted line in (C) was calculated from  $I_{1.4\text{ms}} - (0.42 \times R + 0.58 \times O)$ . The solid traces in (B) and (D) are the single exponential fits to the data; the upright and inverted triangles indicate the absorbance level at  $t=0$  (obtained by extrapolating the kinetic traces back to time zero) and that of the **R** state, respectively. The diamond in (D) is the absorbance level of the **O** state obtained at 280 ms.

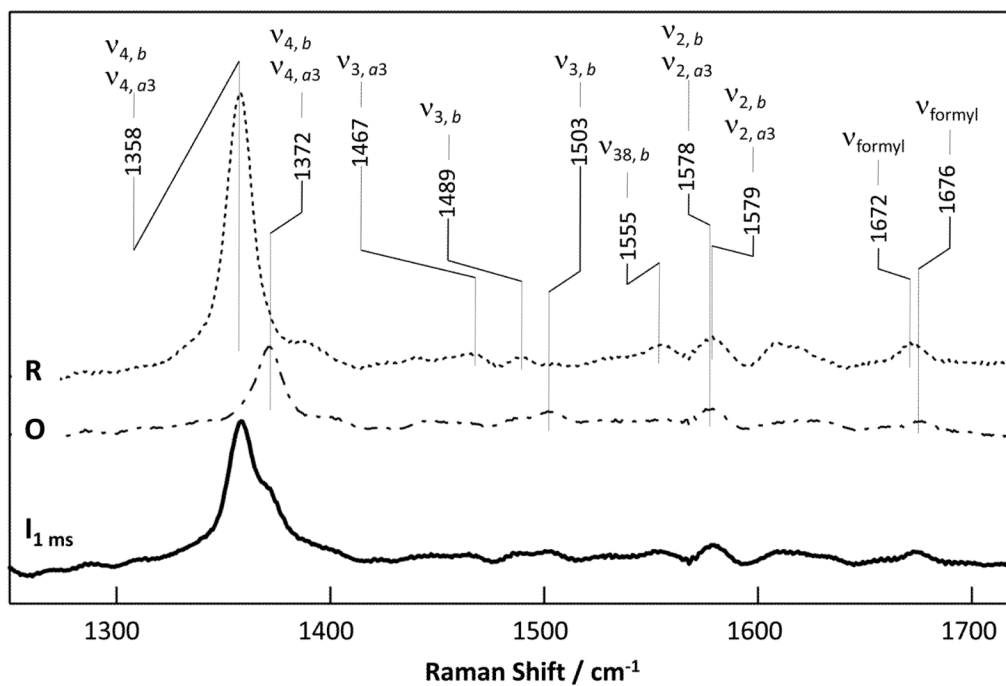


**Figure 2.** The RR spectrum obtained at 1 ms following the mixing of the fully reduced  $ba_3$  (**R**) with  $O_2$ -saturated buffer. The RR spectra of the **R** (dotted line) and **O** (dot-dashed line) states of the enzyme are shown as references. The excitation wavelength was 413.1 nm.

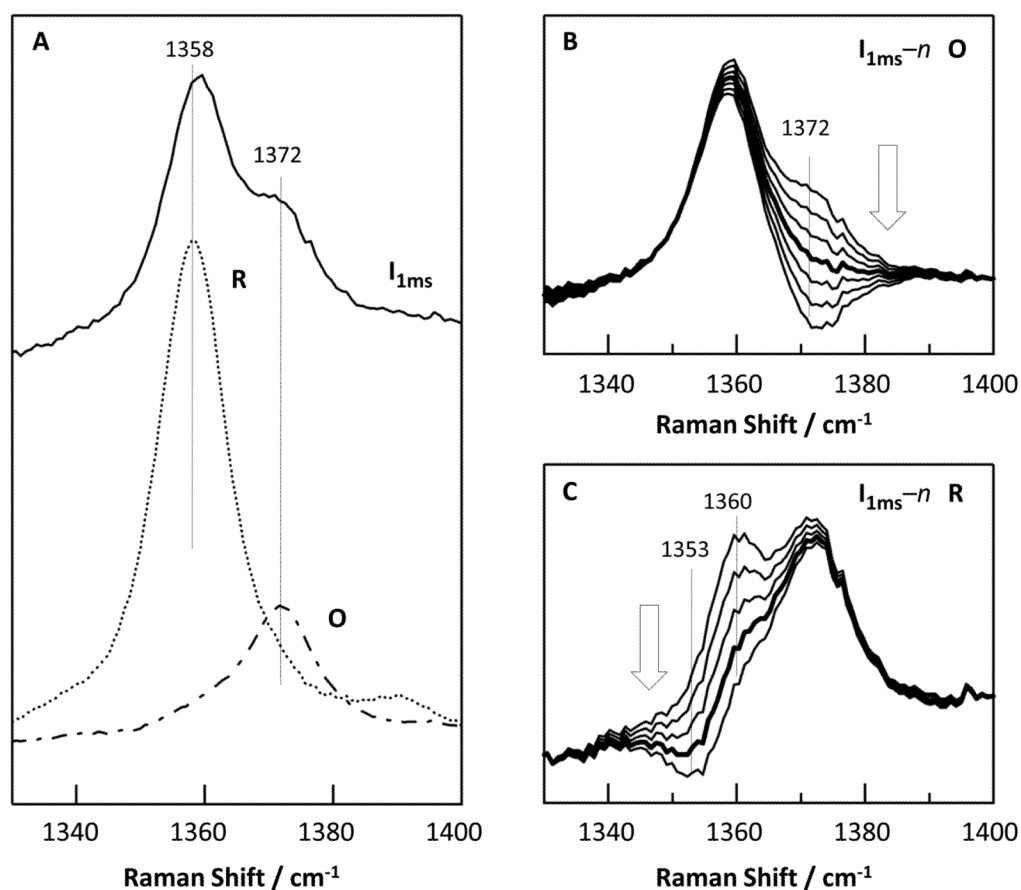


**Figure 3.**

The  $v_4$  bands of the 1 ms intermediate state (solid line) as compared to the **R** (dotted line) and **O** (dot-dashed line) states of  $ba_3$  (A) and the simulated spectra obtained by subtracting increasing amount of the **O** or **R** spectrum from the 1 ms RR spectrum (as indicated by the arrows) (B–C). The thick line in (B) shows the best simulated spectrum with the spectral contribution from the **O** state totally canceled. The thick line in (C) demonstrates a shift of the  $v_4$  band to higher frequency in the 1 ms spectrum with respect to that of the equilibrium **R** state.

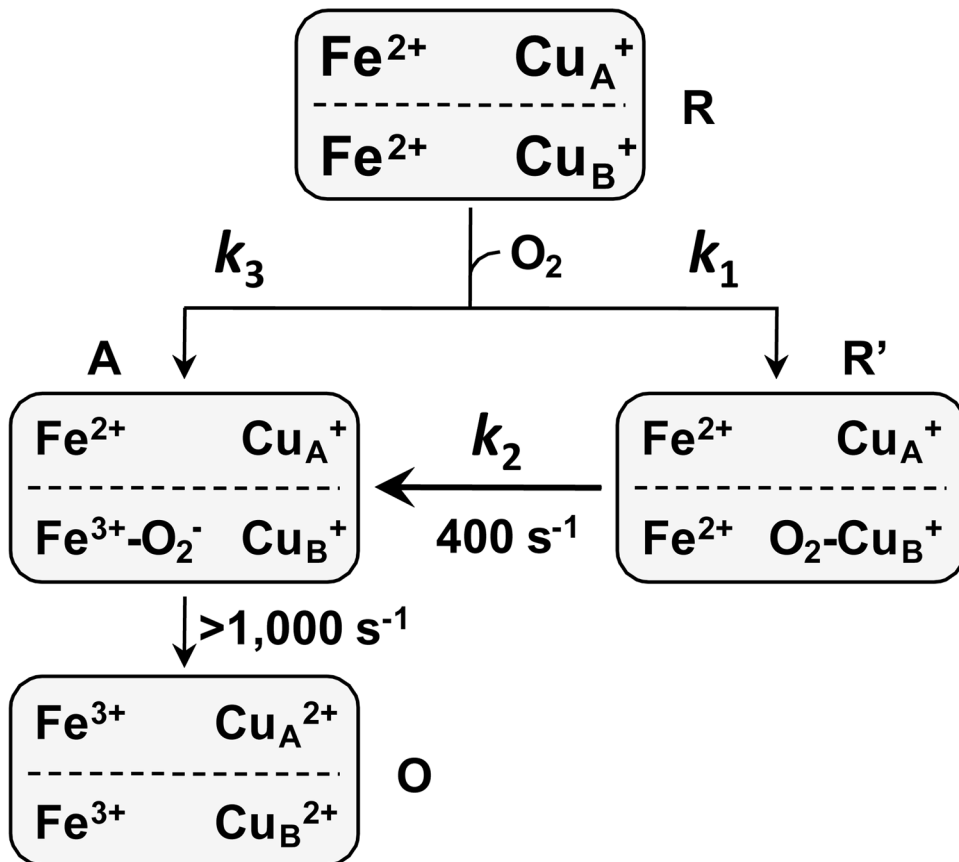


**Figure 4.**  
The bifurcated oxygen reaction mechanism of the *ba<sub>3</sub>* enzyme.